A Majorana fermion *t* - *J* model in one dimension

1997 J. Phys.: Condens. Matter 9 7963

(http://iopscience.iop.org/0953-8984/9/38/005)

J. Phys.: Condens. Matter **9** (1997) 7963–7979. Printed in the UK PII: S0953-8984(97)85848-1

A Majorana fermion t–J model in one dimension

Diptiman Sen†§ and B Sriram Shastry‡‖

† Centre for Theoretical Studies, Indian Institute of Science, Bangalore 560012, India

‡ Physics Department, Indian Institute of Science, Bangalore 560012, India

Received 10 July 1997

Abstract. We study a rotation-invariant Majorana fermion model in one dimension using diagrammatic perturbation theory and numerical diagonalization of small systems. The model is inspired by a Majorana representation of the antiferromagnetic spin-$\frac{1}{2}$ chain, and it is similar in form to the t–J model of electrons, except that the Majorana fermions carry spin 1 and Z_2 charge. We discuss the implications of our results for the low-energy excitations of the spin-$\frac{1}{2}$ chain. We also discuss a generalization of our model from three species of Majorana fermions to N species; the SO(4) symmetric model is particularly interesting.

1. Introduction

In a recent paper [1], we used a representation of spin $\frac{1}{2}$ in terms of three species of Majorana fermions [2, 3] in order to study the antiferromagnetic spin-$\frac{1}{2}$ chain. The Majorana representation has an advantage over other representations (such as the Schwinger boson or fermion representations [4, 5]) in that one does not have to impose a constraint on the total particle number at each site (see however reference [6]). It is also rotation invariant unlike the 'drone fermion' and the Holstein–Primakoff boson representations [7, 8].

For the spin-$\frac{1}{2}$ chain with isotropic nearest-neighbour interactions, the Majorana representation followed by a rotation-invariant Hartree–Fock (H–F) analysis [1] leads to a picture of the low-energy excitations of the spin-$\frac{1}{2}$ chain which is qualitatively similar to that obtained by other methods [9–11]. In particular, we find that the excitations are described by a two-parameter continuum in the (q, ω) space; for each momentum q, the low-energy spectrum has a range of energies ω as if the excitations are made up of two particles (called 'spinons'). We also get reasonable dynamic structure functions and susceptibilities at all temperatures if we introduce some phenomenological structure functions. We should note however that our Majorana fermions carry spin 1 unlike the 'standard' spinons with spin $\frac{1}{2}$.

The positive features of the Majorana representation encourage us to study the fluctuations about the H–F state of the spin-$\frac{1}{2}$ chain. More generally, it seems to be interesting to examine a strongly correlated Majorana fermion model in one dimension and contrast its properties with much better-studied electronic systems like the Hubbard model. Such an analysis would also be useful for other possible applications of Majorana fermions such as the Kondo problem [2]. In this paper, we therefore study the t–J model with Majorana fermions; the electronic version of this model has played a major role in theories of strongly correlated systems like the high-temperature superconductors.

§ E-mail address: diptiman@cts.iisc.ernet.in

‖ E-mail address: bss@physics.iisc.ernet.in

The outline of our paper is as follows. In section 2, we briefly recall the Majorana representation of spin $\frac{1}{2}$ and the H–F analysis of the antiferromagnetic chain given in our earlier paper [1]. This motivates a study of the t–J model which is introduced in section 3. We present the Feynman rules for the propagator and the vertex, and compute the one-loop correction to the propagator. In section 4.1, we compute the two-loop correction to the propagator; we find the remarkable result that the on-shell correction is of the same form as the tree-level dispersion relation. In section 4.2, we compute the two-loop correction to the dynamic structure function. The result can be used to perturbatively improve the power law of the equal-time correlation function and the ground-state energy of the spin-$\frac{1}{2}$ chain from the values obtained at the H–F level. In section 4.3, we study the one-loop correction to the vertex. In section 5, we discuss the symmetries of the t–J model and numerically analyse the spectrum of small systems using exact diagonalization. In section 6, we generalize our model from SO(3) to SO(N), and we briefly examine the SO(4) case which is particularly interesting. Finally, in section 7, we summarize our understanding of the t–J model.

2. Majorana fermions and the antiferromagnetic spin-$\frac{1}{2}$ chain

At each site n, the spin operators $\boldsymbol{S}_n = \boldsymbol{\sigma}_n/2$ can be written in terms of the Majorana operators $\boldsymbol{\phi}_n$ as [1, 2, 3]

$$\sigma_n^x = -\mathrm{i}\phi_n^y\phi_n^z \qquad \sigma_n^y = -\mathrm{i}\phi_n^z\phi_n^x \qquad \sigma_n^z = -\mathrm{i}\phi_n^x\phi_n^y. \tag{1}$$

(We set Planck's constant equal to 1.) The Hermitian operators ϕ_n^a (with $a = x, y, z$) satisfy the anticommutation relations

$$\{\phi_m^a, \phi_n^b\} = 2\delta_{mn}\delta_{ab}. \tag{2}$$

Note that there is a local Z_2 gauge invariance, since changing the sign of $\boldsymbol{\phi}_n$ does not affect $\boldsymbol{S}_n$. We will therefore say that $\boldsymbol{\phi}_n$ (or any odd power of it) carries a Z_2 charge. Let us define the trilinear and Hermitian object $\psi_n = -\mathrm{i}\phi_n^x\phi_n^y\phi_n^z$. Then $[\sigma_m^a, \psi_n] = 0$, and $\{\psi_m, \psi_n\} = 2\delta_{mn}$. Under rotations, $\boldsymbol{\phi}_n$ and $\boldsymbol{\sigma}_n$ transform like vectors (spin-1 objects), while ψ_n remains invariant. On the other hand, ψ_n carries a Z_2 charge while $\boldsymbol{\sigma}_n$ is Z_2 neutral. Thus we have two different composite operators, $\boldsymbol{\sigma}_n$ and ψ_n, which carry spin and charge respectively.

For a system with L sites, it is known that the minimum possible dimension which allows a representation of the form given in equations (1) and (2) is $2^{L+[L/2]}$, where $[L/2]$ denotes the largest integer less than or equal to $L/2$. For L sites with a spin-$\frac{1}{2}$ object at each site, the Hilbert space clearly has dimension 2^L. Thus the Majorana representation of spin-$\frac{1}{2}$ objects requires us to enlarge the space of states; the complete Hilbert space of states is given by a direct product of a 'physical' space and an 'unphysical' one. The operators $\boldsymbol{\sigma}_n$ act only on the physical states, while the $\boldsymbol{\phi}_n$ mix up different unphysical states.

We now consider the Heisenberg antiferromagnetic chain with the Hamiltonian

$$H = J\sum_n \boldsymbol{S}_n \cdot \boldsymbol{S}_{n+1} \tag{3}$$

where $J > 0$. We use periodic boundary conditions $\boldsymbol{S}_{L+1} = \boldsymbol{S}_1$. The spectrum of (3) is exactly solvable by the Bethe *ansatz*; the ground-state energy per site for large L is given by $E_0/L = (-\ln 2 + 1/4)J = -0.4431J$. The lowest excitations are known to be fourfold degenerate, consisting of a triplet ($S = 1$) and a singlet ($S = 0$) [10]. The excitation spectrum is described by a two-parameter continuum in the (q, ω) space, where

$-\pi < q \leqslant \pi$. The lower boundary of the continuum is described by the des Cloiseaux–Pearson relation [9]

$$\omega_l(q) = \frac{\pi J}{2}|\sin q| \tag{4}$$

while the upper boundary is given by

$$\omega_u(q) = \pi J\left|\sin\frac{q}{2}\right|. \tag{5}$$

We can understand this continuum by thinking of these excitations as being made up of two spin-$\frac{1}{2}$ objects ('spinons') with the dispersion [10]

$$\omega_s(q) = \frac{\pi J}{2}\sin q \tag{6}$$

where $0 < q < \pi$. A triplet (or a singlet) excitation with momentum q is made up of two spinons with momenta q_1 and q_2, such that $0 < q_1 \leqslant q_2 < \pi$, $q = q_1 + q_2$, and $\omega(q) = \omega_s(q_1) + \omega_s(q_2)$.

The Majorana analysis of this system proceeds as follows [1]. We write (3) in terms of Majorana operators and then perform a H–F decomposition. Thus

$$\begin{aligned} H &= -\frac{J}{4}\sum_n(\phi_n^x\phi_n^y\phi_{n+1}^x\phi_{n+1}^y + \text{cyclic permutations of } (x,y,z)) \\ &\simeq \frac{J}{4}\sum_n[\phi_n^x\phi_{n+1}^x\langle\phi_n^y\phi_{n+1}^y\rangle + \langle\phi_n^x\phi_{n+1}^x\rangle\phi_n^y\phi_{n+1}^y \\ &\quad - \langle\phi_n^x\phi_{n+1}^x\rangle\langle\phi_n^y\phi_{n+1}^y\rangle + \text{cyclic permutations of } (x,y,z)]. \end{aligned} \tag{7}$$

For a rotation- and translation-invariant H–F analysis, we have $g = \mathrm{i}\langle\phi_n^a\phi_{n+1}^a\rangle$, where g has the same value for all n and $a = x, y, z$. (Our earlier paper [1] follows slightly different conventions.) The Fourier expansion of ϕ_n is defined as

$$\phi_n^a = \sqrt{\frac{2}{L}}\sum_{0<q<\pi}[b_{aq}\mathrm{e}^{\mathrm{i}qn} + b_{aq}^\dagger\mathrm{e}^{-\mathrm{i}qn}] \tag{8}$$

where $\{b_{aq}, b_{bq'}^\dagger\} = \delta_{ab}\delta_{qq'}$. We will work with *antiperiodic* boundary conditions for ϕ_n^a and *even* values of L in order to eliminate modes with q equal to 0 and π. In equation (8), $q = 2\pi(p-1/2)/L$, with $p = 1, 2, \ldots, L/2$. In the limit $L \to \infty$, we get

$$H = \sum_a\sum_{0<q<\pi}\omega_q b_{aq}^\dagger b_{aq} + 3LJ\left(\frac{g^2}{4} - \frac{g}{\pi}\right) \tag{9}$$

where the Majorana fermions have the dispersion $\omega_q = v\sin q$, with $v = 2gJ$. The value of g is determined self-consistently to be $g = 2/\pi$. The H–F ground-state energy is therefore

$$\frac{E_{0\,HF}}{L} = -\frac{3}{\pi^2}J = -0.3040J \tag{10}$$

which is greater than the exact value mentioned above. The 'spinon' spectrum has the same form as in (6), except that we get $v = 4J/\pi$ instead of $v_{exact} = \pi J/2$.

We can go on to show that the Majorana fermion has spin 1, and a two-fermion state therefore has $S = 0$, 1, or 2 in general. However, the state created by $S_q^z = \sum_n S_n^z\mathrm{e}^{-\mathrm{i}qn}$, where $0 < q < \pi$, has the form

$$S_q^z|0\rangle = -\mathrm{i}\sum_{\pi-q<k<\pi} b_{x,k}^\dagger b_{y,q-k}^\dagger|0\rangle \tag{11}$$

and has $S = 1$. We thus obtain a two-parameter continuum of triplet excitations as in equations (4) and (5), with a prefactor $4/\pi$ instead of $\pi/2$.

Finally, the equal-time two-spin correlation function is given by

$$G_n \equiv \langle 0|\boldsymbol{S}_n \cdot \boldsymbol{S}_0|0\rangle = \begin{cases} \dfrac{3}{4} & \text{for } n = 0 \\ -\dfrac{3}{2\pi^2 n^2}[1-(-1)^n] & \text{for } n \neq 0. \end{cases} \tag{12}$$

This does not agree with the correct asymptotic behaviour of G_n which is known to oscillate as $(-1)^n/n$. In particular, the H–F static structure function $S(q) = \sum_n G_n \mathrm{e}^{-\mathrm{i}qn}$ does not diverge as $q \to \pi$ in contrast to the correct $S(q)$ which has a logarithmic divergence at π. (Note that we do get $\sum_n G_n = 0$, as expected for a singlet ground state.) We will show in section 4.2 that two-loop effects effectively reduce the power governing the asymptotic decay from 2 to 1.75, which is somewhat closer to the correct value of 1. At the same time, the ground-state energy per site is reduced from $-0.3040J$ to $-0.3338J$, which is also closer to the Bethe *ansatz* value of $-0.4431J$.

One can now consider fluctuations about the H–F ground state by doing loop calculations. However, instead of studying only the Hamiltonian (7) as is sufficient for the spin-$\frac{1}{2}$ chain, it is useful to study a more general model which has the same structure but has two parameters instead of one; the parameters are a hopping amplitude t and a quartic interaction J. This is the subject of the following sections.

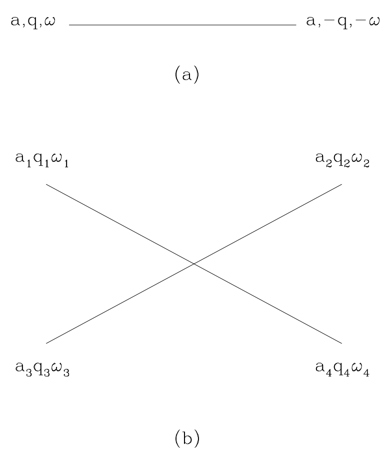

Figure 1. The propagator and vertex for the Majorana t–J model.

3. The Majorana t–J model

We consider the Hamiltonian

$$H = \frac{-\mathrm{i}t}{4}\sum_{a,n}\phi_n^a\phi_{n+1}^a - \frac{J}{4}\sum_n(\phi_n^x\phi_n^y\phi_{n+1}^x\phi_{n+1}^y + \text{cyclic permutations of } (x,y,z)) \tag{13}$$

with t chosen to be positive, and we perform a perturbative expansion with the quartic term. To begin the diagrammatic analysis, we generalize the Fourier expression (8) to the interaction picture field

$$\phi_n^a(t) = \sqrt{\frac{2}{L}} \sum_{-\pi<q<\pi} \phi_q^a e^{i(qn-\omega_q t)} \tag{14a}$$

where

$$\phi_q^a = \begin{cases} b_{aq} & \text{if } 0 < q < \pi \\ b_{a,-q}^\dagger & \text{if } -\pi < q < 0 \end{cases} \tag{14b}$$

with

$$\omega_q = t \sin q \tag{15}$$

for all q. Then we obtain the propagator

$$\langle 0|T\phi_q^a(t)\phi_{-q}^b(0)|0\rangle \equiv iG^{ab}(q,t) = i\delta^{ab}G(q,t) \tag{16a}$$

and

$$iG(q,\omega) = i\int_{-\infty}^{\infty} dt\ G(q,t)e^{i\omega t} = \frac{i}{\omega - \omega_q + i\eta\theta(q)} \tag{16b}$$

where η is infinitesimal and positive, and $\theta(q) = 1$ if $0 < q < \pi$ and -1 if $-\pi < q < 0$. For loop calculations, it is convenient to define a propagator even for values of q not lying in the range $[-\pi,\pi]$. To do this, we first define a momentum $\underline{q} = q + 2n\pi$ where the integer n is chosen such that $-\pi < \underline{q} \leqslant \pi$. Then we *define* $G(q,\omega) = G(\underline{q},\omega)$ using (16). The propagator is shown by a solid line in figure 1(a).

The vertex shown in figure 1(b) is obtained by Fourier transforming the quartic term in (13). The Feynman rule for the vertex is found to be

$$\begin{aligned} i\Gamma&(a_1,q_1,\omega_1;a_2,q_2,\omega_2;a_3,q_3,\omega_3;a_4,q_4,\omega_4) \\ &= i(2\pi)^2\delta_P\left(\sum_i q_i\right)\delta\left(\sum_i \omega_i\right)4J\cos\left(\frac{1}{2}\sum_i q_i\right) \\ &\quad\times\left[\delta^{a_1a_2}\delta^{a_3a_4}\sin\left(\frac{1}{2}(q_1-q_2)\right)\sin\left(\frac{1}{2}(q_3-q_4)\right)\right. \\ &\quad\left. + \text{cyclic permutations of } (a_2,q_2;a_3,q_3;a_4,q_4)\right] \end{aligned} \tag{17}$$

where the spin indices a_1 to a_4 can take the values x, y, z, and the momenta q_1 to q_4 need not lie in the range $[-\pi,\pi]$. The periodic δ-function is defined as

$$\delta_P(q) = \sum_{n=-\infty}^{\infty} \delta(q - 2n\pi). \tag{18}$$

The expression in (17) is antisymmetric under the exchange of any two labels (a_i,q_i,ω_i) and (a_j,q_j,ω_j); it also vanishes if all of the indices a_i are equal.

We now compute the simplest loop effect, namely, the one-loop contribution to the propagator shown in figure 2(a). It is called a one-loop contribution because there is one energy–momentum that we have to integrate over. To this order in J, the self-energy is found to have the energy-independent form

$$\Sigma^{(1)}(q,\omega) = \frac{4J}{\pi}\sin q \tag{19}$$

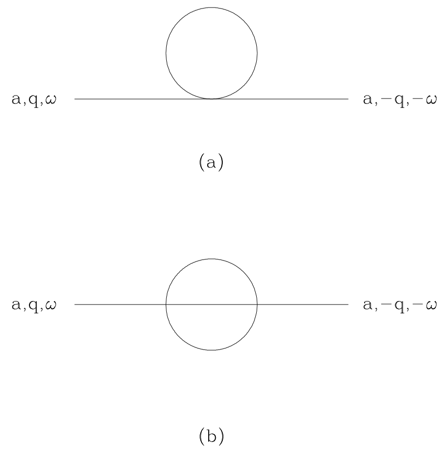

Figure 2. The one- and two-loop contributions to the propagator.

where the superscript (1) denotes the order of the loop. Thus the dispersion relation changes from (15) to

$$\omega_q = \left(t + \frac{4J}{\pi} \right) \sin q . \tag{20}$$

We will therefore use the expression (20) in the propagator (16) for all of the loop calculations below. Note that we can recover the antiferromagnetic spin-$\frac{1}{2}$ chain by setting $t = 0$ in (13); equation (20) then gives us precisely the H–F dispersion discussed in section 2.

4. Loop calculations

4.1. The two-loop contribution to the propagator

We will now compute the two-loop diagram shown in figure 2(b). The two energy integrations can be easily carried out using the identities

$$\begin{aligned} \int_{-\infty}^{\infty} \frac{\mathrm{d}\omega}{2\pi} \; \frac{1}{\omega - \alpha + \mathrm{i}\eta} \frac{1}{\omega - \beta - \mathrm{i}\eta} &= \frac{\mathrm{i}}{\beta - \alpha + \mathrm{i}\eta} \\ \int_{-\infty}^{\infty} \frac{\mathrm{d}\omega}{2\pi} \; \frac{1}{\omega - \alpha + \mathrm{i}\eta} \frac{1}{\omega - \beta + \mathrm{i}\eta} &= 0 \end{aligned} \tag{21}$$

if α and β are real.

We then obtain the following expression for the self-energy:

$$\Sigma^{(2)}(q, \omega) = -\frac{4J^2}{\pi^2} \int_{-\pi}^{\pi} \int_{-\pi}^{\pi} \mathrm{d}l_1 \; \mathrm{d}l_2 \; \frac{\sin^2[q + \frac{1}{2}(l_1 + l_2)] \sin^2[\frac{1}{2}(l_1 - l_2)]}{\omega + \omega_{l_1} + \omega_{l_2} - \omega_{l_1 + l_2 + q} \pm \mathrm{i}\eta} \tag{22}$$

where we take the upper sign ($\mathrm{i}\eta$) in the denominator if

$$-\pi < l_1, l_2 < 0 \qquad \text{and} \qquad 0 < \underline{l_1 + l_2 + q} < \pi$$

and we take the lower sign ($-\mathrm{i}\eta$) if

$$0 < l_1, l_2 < \pi \qquad \text{and} \qquad -\pi < \underline{l_1 + l_2 + q} < 0.$$

It is clear at this point that

$$\Sigma^{(2)}(-q,-\omega) = \Sigma^{(2)}(q,\omega). \tag{23}$$

This property of the self-energy can be shown to be true to all orders in J. Furthermore, $\Sigma^{(2)}(\pi - q,\omega) = \Sigma^{(2)}(q,\omega)$. Now let us choose $0 < q < \pi$ and find the on-shell dispersion relation to order J^2, namely,

$$\omega = \left(t + \frac{4J}{\pi}\right)\sin q + \Sigma^{(2)}(q,\omega). \tag{24}$$

To this order in J, we can set $\omega = (t + 4J/\pi)\sin q$ in the second term on the right-hand side of (24) or, equivalently, in the denominator of (22). We then find that the denominator in (22) never crosses zero in the given ranges of l_1 and l_2; thus we can drop the $\pm \mathrm{i}\eta$ and the integrals are purely real. We then *numerically* find that (22) has the remarkably simple form

$$\Sigma^{(2)}\left(q, \left(t + \frac{4J}{\pi}\right)\sin q\right) = -0.467\frac{4J^2}{\pi^2(t + 4J/\pi)}\sin q \tag{25}$$

for all q in the range $[0,\pi]$. Thus the dispersion relation to order J^2 is

$$\omega = \left(t + \frac{4J}{\pi} - 0.189\frac{J^2}{t + 4J/\pi}\right)\sin q. \tag{26}$$

We find it surprising that the form of the dispersion relation remains the same even at the two-loops level, and suspect that this may be true to all orders in J.

4.2. *The two-loop contribution to dynamic structure function*

We will compute the two-spin correlation function

$$S_{zz}(q,\omega) \equiv \text{Fourier transform of } \langle 0|S_n^z(t)S_0^z(0)|0\rangle \tag{27}$$

to two loops. To any order, we can show that this function remains invariant under $(q,\omega) \to (-q,-\omega)$. We can obtain the static structure function (equal-time correlation function) $S_{zz}(q)$ by integrating:

$$S_{zz}(q) = \int_{-\infty}^{\infty}\frac{\mathrm{d}\omega}{2\pi}\; S_{zz}(q,\omega)\mathrm{e}^{\mathrm{i}\omega t} \tag{28}$$

and taking the limit $t \to 0^+$. This is a function of $|q|$, so it is sufficient to compute it for $0 < q < \pi$.

The lowest-order result for the correlation function is obtained from the one-loop diagram in figure 3(a). After carrying out the energy integration, we obtain

$$S_{zz}^{(1)}(q,\omega) = \begin{cases} \dfrac{\mathrm{i}}{2\pi}\displaystyle\int_{-\pi}^{\pi}\mathrm{d}l_1\;\frac{1}{\omega - \omega_{l_1} - \omega_{q-l_1} + \mathrm{i}\eta} & \text{if } 0 < l_1, \underline{q - l_1} < \pi \\[2ex] \dfrac{\mathrm{i}}{2\pi}\displaystyle\int_{-\pi}^{\pi}\mathrm{d}l_1\;\frac{1}{\omega_{l_1} + \omega_{q-l_1} - \omega + \mathrm{i}\eta} & \text{if } -\pi < l_1, \underline{q - l_1} < 0\ . \end{cases} \tag{29}$$

For $-\pi < q < \pi$, we then obtain

$$S_{zz}^{(1)}(q) = \frac{|q|}{2\pi}. \tag{30}$$

The Fourier transform of this gives the spatial correlation function in (12).

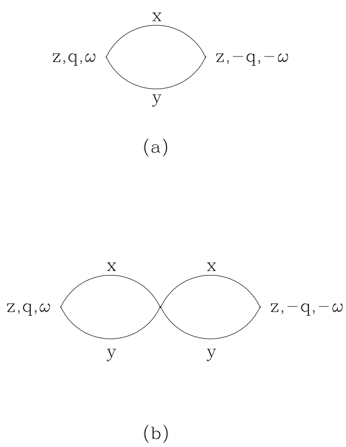

Figure 3. The one- and two-loop contributions to the two-spin correlation function.

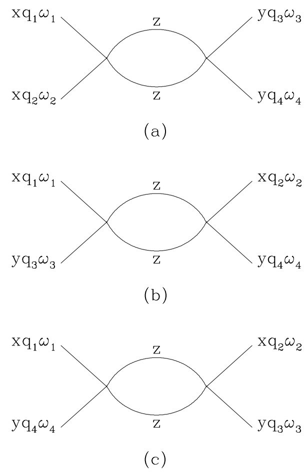

Figure 4. The one-loop contributions to the vertex.

At the two-loops level, we have to compute the diagram given in figure 3(b). After performing the two energy integrations, we arrive at the expression

$$S_{zz}^{(2)}(q,\omega) = \frac{\mathrm{i}J}{4\pi^2}\int_{-\pi}^{\pi}\int_{-\pi}^{\pi}\mathrm{d}l_1\ \mathrm{d}l_2\ \sin\left[\frac{1}{2}(l_1+l_2)\right]\sin\left[q+\frac{1}{2}(l_1+l_2)\right]$$
$$\times\begin{cases} \dfrac{1}{(e_1-\mathrm{i}\eta)(e_2-\mathrm{i}\eta)} & \text{if } 0<l_1,l_2,-(\underline{l_1+q}),-(\underline{l_2+q})<\pi \\ \dfrac{1}{(e_1+\mathrm{i}\eta)(e_2+\mathrm{i}\eta)} & \text{if } 0<-l_1,-l_2,\underline{l_1+q},\underline{l_2+q}<\pi \\ \dfrac{-1}{(e_1-\mathrm{i}\eta)(e_2+\mathrm{i}\eta)} & \text{if } 0<l_1,-l_2,-(\underline{l_1+q}),\underline{l_2+q}<\pi \\ \dfrac{-1}{(e_1+\mathrm{i}\eta)(e_2-\mathrm{i}\eta)} & \text{if } 0<-l_1,l_2,\underline{l_1+q},-(\underline{l_2+q})<\pi \end{cases} \tag{31a}$$

where

$$e_1 = \omega + \omega_{l_1} - \omega_{l_1+q} \tag{31b}$$
$$e_2 = \omega + \omega_{l_2} - \omega_{l_2+q}. \tag{31c}$$

We then get, for $0<q<\pi$,

$$\begin{aligned} S_{zz}^{(2)}(q) &= -\frac{J}{2\pi^2(t+4J/\pi)}I(q) \\ I(q) &= \int_0^q\int_0^q \mathrm{d}l_1\ \mathrm{d}l_2\ \frac{\cos[\frac{1}{2}(l_1+l_2)]\cos[q-\frac{1}{2}(l_1+l_2)]}{\sin l_1+\sin l_2+\sin(q-l_1)+\sin(q-l_2)}. \end{aligned} \tag{32}$$

We find analytically that $I(q)$ vanishes as $q\to 0$, and numerically that

$$\int_0^{\pi}\mathrm{d}q\ I(q) = 0. \tag{33}$$

These are consistency checks following from the facts that the ground state is a singlet and that the two-spin correlation at the same spatial point is equal to 3/4; we already know that the one-loop correlation in equation (12) satisfies these checks.

We now use equation (32) to derive some interesting numbers relating to the antiferromagnetic spin-$\frac{1}{2}$ chain. First of all, we can show analytically that $I(q)$ is finite for all q, while $I'(q)$ diverges logarithmically at $q = \pi$ with coefficient 1; that is,

$$\begin{aligned} I'(q) &= \ln|\pi - q| + \text{nondivergent terms} \\ I(q) &= I(\pi) + (q-\pi)\ln|\pi - q| \qquad \text{as } q \to \pi. \end{aligned} \tag{34}$$

At long distances, the leading term in the spatial correlation function $G_n = 3\langle 0|S_n^z S_0^z|0\rangle$ takes the form

$$\int_0^\pi \frac{\mathrm{d}q}{\pi}\ I(q)\cos(qn) = -\frac{(-1)^n}{\pi n^2}\ln n + \mathrm{O}\left(\frac{1}{n^2}\right) \qquad \text{as } n \to \infty. \tag{35}$$

After adding this to the one-loop result, we see that the long-distance correlation function has an oscillatory term going as

$$G_n = (-1)^n \frac{3}{2\pi^2 n^2}\left[1 + \frac{J}{\pi(t + 4J/\pi)}\ln n + \cdots\right] \tag{36}$$

where the dots indicate contributions from more than two loops. If we now *assume* that these higher-order terms come with the right numerical factors to turn the sum into an exponential series, we see that the long-distance correlation decays as $(-1)^n n^{-\alpha}$, where the exponent α goes as

$$\alpha = 2 - \frac{J}{\pi(t + 4J/\pi)} \tag{37}$$

to order J. For the spin-$\frac{1}{2}$ chain, we must set $t = 0$; this gives $\alpha = 1.75$ to this order.

The second interesting number for the spin-$\frac{1}{2}$ chain which we can derive from (32) is the ground-state energy per site; this is equal to JG_1 for $t = 0$. On numerically integrating (32), we find the two-loop result

$$G_1^{(2)} = -\frac{3}{8\pi^2}\int_0^\pi \mathrm{d}q\ I(q)\cos q = -0.0298. \tag{38}$$

On adding this to the one-loop result, we get the value $-0.3338J$.

4.3. The one-loop contribution to the vertex

For completeness, we will mention the one-loop correction to the vertex. Let us choose two of the spin indices to be x and two to be y. From (17), the zero-loop form of the vertex is given by $(2\pi)^2$ times the energy–momentum-conserving δ-functions multiplied by

$$\mathrm{i}\Gamma^{(0)} = \mathrm{i}\,4J\cos\left(\frac{1}{2}\sum_i q_i\right)\sin\left(\frac{1}{2}(q_1 - q_2)\right)\sin\left(\frac{1}{2}(q_3 - q_4)\right). \tag{39}$$

The one-loop correction $\mathrm{i}\Gamma^{(1)}(x, q_1, \omega_1; x, q_2, \omega_2; y, q_3, \omega_3; y, q_4, \omega_4)$ is given by the sum of the three diagrams shown in figure 4. On carrying out the energy integration, we find that the contribution of figure 4(a) is

$$\begin{aligned} &-\mathrm{i}\,8J^2\cos\left(\frac{1}{2}\sum_i q_i\right)\sin\left(\frac{1}{2}(q_1 - q_2)\right)\sin\left(\frac{1}{2}(q_3 - q_4)\right)\int_{-\pi}^{\pi}\frac{\mathrm{d}l}{2\pi}\ \sin^2\left[l + \frac{1}{2}(q_1 + q_2)\right] \\ &\qquad \times \begin{cases} \dfrac{1}{\omega_{l+q_1+q_2} - \omega_l - \omega_1 - \omega_2 + \mathrm{i}\eta} & \text{if } 0 < l, -(\underline{l + q_1 + q_2}) < \pi \\ \dfrac{1}{\omega_l + \omega_1 + \omega_2 - \omega_{l+q_1+q_2} + \mathrm{i}\eta} & \text{if } 0 < -l, \underline{l + q_1 + q_2} < \pi. \end{cases} \end{aligned} \tag{40}$$

The contribution of figure 4(b) can be obtained from equation (40) by changing the coefficient 8 to 16 and cyclically replacing $q_2 \to q_3 \to q_4 \to q_2$ and $\omega_2 \to \omega_3$. The contribution of figure 4(c) can be obtained from equation (40) by changing 8 to 16 and replacing $q_2 \to q_4 \to q_3 \to q_2$ and $\omega_2 \to \omega_4$.

5. Symmetries and numerical results

5.1. Numerical results

We can numerically study the spectrum of our model by means of the exact diagonalization of small systems. To do that, it is useful to know all the symmetries of the model. Some of the conserved quantum numbers are the total spin $\boldsymbol{S}^2$ and any one of its components, say, S_z, the total momentum q modulo 2π, and parity $P = \pm 1$ which arises from the symmetry of the Hamiltonian under

$$\phi_n \to (-1)^n \phi_{L+1-n}. \tag{41}$$

In addition, there is a Z_2 quantum number defined as follows. Consider

$$\Gamma = \begin{cases} \psi_1 \psi_2 \cdots \psi_L & \text{if } \dfrac{L}{2} \text{ is even} \\ \mathrm{i}\psi_1 \psi_2 \cdots \psi_L & \text{if } \dfrac{L}{2} \text{ is odd} \end{cases} \tag{42}$$

satisfying $\Gamma^\dagger = \Gamma^{-1} = \Gamma$. This operator anticommutes with each of the ϕ_n and therefore commutes with the Hamiltonian (13). Hence the eigenvalue of $\Gamma = \pm 1$ is a good quantum number. We will *define* $\Gamma = 1$ for the ground state of the t–J model; we can ensure this by introducing a minus sign in the definition (42) if necessary.

There are a few selection rules and energy degeneracies connecting some of these quantum numbers. We will see below that the ground state has $q = 0$, and we choose $\Gamma = 1$. We can now obtain various excited states by acting on it with a certain number of Majorana operators as defined in (8). Each such operator carries a momentum q which is an *odd* multiple of π/L, and $\Gamma = -1$. It is therefore clear that all states must have $\Gamma = \exp(\mathrm{i}qL)$; this eigenvalue is 1 or -1 depending on whether the state has an even or odd number of Majorana fermions. Secondly, Majorana operators with momenta q and $\pi - q$ carry the same energy by parity. Thus states with an odd number of Majorana operators, i.e. with $\Gamma = -1$, must have an energy degeneracy between total momenta equal to q and $\pi - q$. States with $\Gamma = 1$ must have an energy degeneracy between momenta q and $-q$.

For a numerical study, it is more convenient to rewrite (13) in the form

$$H = \frac{1}{4} \sum_{n=1}^{L} (-\mathrm{i}t\psi_n \psi_{n+1} + J) \boldsymbol{\sigma}_n \cdot \boldsymbol{\sigma}_{n+1}. \tag{43}$$

As mentioned in section 2, we use periodic boundary conditions for $\boldsymbol{\sigma}_n$ and antiperiodic ones for ψ_n. We diagonalize H in a basis consisting of a direct product of states of the form $|\Psi_i\rangle \otimes |\alpha_j\rangle$, such that the operators $\boldsymbol{\sigma}_n$ and ψ_n act only on $|\Psi_i\rangle$ and $|\alpha_j\rangle$ respectively. In order to study the spectral flow from the pure-J model to the pure-t model, we introduce a parameter x lying between 0 and 1, such that $J = 4(1 - x)$ and $t = 4x$. Thus

$$H(x) = \sum_{n=1}^{N} (1 - x - \mathrm{i}x\psi_n \psi_{n+1}) \boldsymbol{\sigma}_n \cdot \boldsymbol{\sigma}_{n+1}. \tag{44}$$

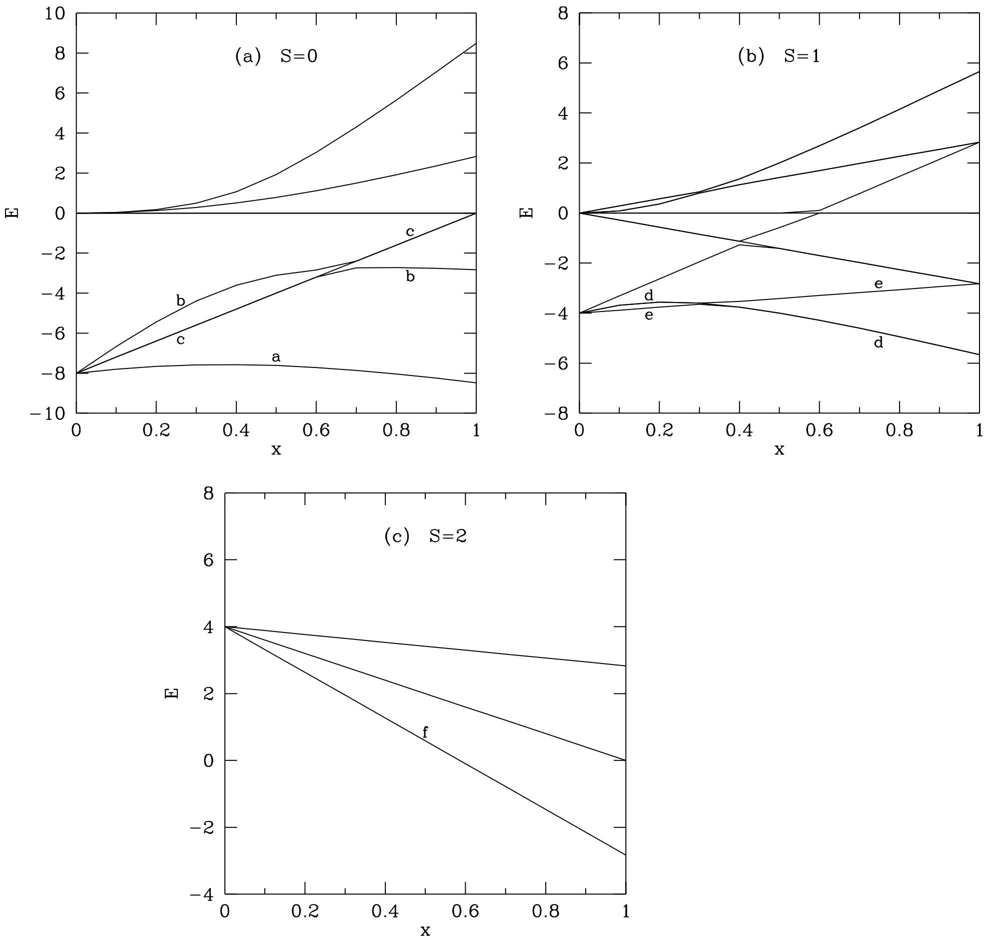

Figure 5. Energies for $L = 4$. $x = 0$ and 1 denote the pure-J and pure-t models respectively. Parts (a)–(c) show all of the energies for total $S = 0, 1, 2$, respectively. The curves marked a–f are discussed in the text.

We have obtained the eigenvalues of (44) for $L = 4$ and 6, for 11 equally spaced values of x from 0 to 1. All of the conserved quantities discussed above have discrete eigenvalues; hence these remain invariant as x changes. Numerically, we only kept track of the eigenvalues of total spin $S = 0, 1, \ldots, L/2$ and total $S_z = 0$; whenever necessary, the eigenvalues q, P, and Γ can be deduced by continuity arguments from the exact analytical solutions known at $x = 1$. The energy eigenvalues in each S-sector are shown in figures 5(a)–5(c) for $L = 4$, and the lowest few eigenvalues in each S-sector are shown in figures 6(a)–6(d) for $L = 6$. We should remark here that the degeneracies of the various levels have not been shown, and that we have not distinguished between true crossings and avoided crossings in these figures.

To get a feeling for the elementary excitations, let us discuss the six low-lying states marked a–f on the figures; these include the three lowest states a, b, c with $S = 0$ in figures 5(a) and 6(a), the two lowest states d, e with $S = 1$ in figures 5(b) and 6(b), and the lowest state f with $S = 2$ in figures 5(c) and 6(c). The energy dependence of these six states can be seen to be quite similar for $L = 4$ and 6. The ground state, marked a, is unique for all

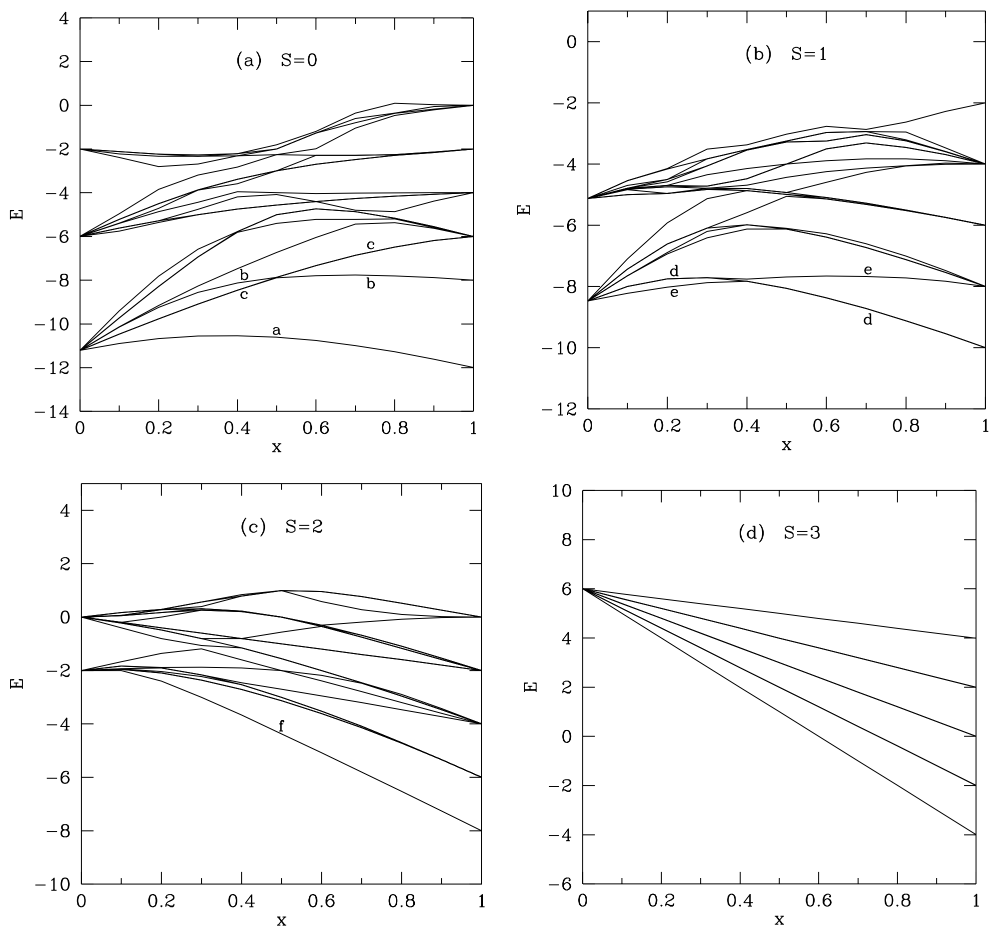

Figure 6. The energy for $L = 6$. Parts (a)–(d) show the lowest 20 energies for $S = 0, 1, 2$, and all the energies for $S = 3$, respectively. The curves marked a–f are discussed in the text.

values of x (except $x = 0$ where it has a degeneracy of $2^{L/2}$); it has spin $S = 0$, momentum $q = 0$, and $\Gamma = 1$. The next two states in the $S = 0$ sector, marked b and c, have $\Gamma = 1$ and -1 with degeneracies of 1 and 2 respectively; these two states exhibit a true level crossing between $x = 0$ and 1, so b is lower than c near $x = 1$ and vice versa near $x = 0$. The two states with $S = 1$, marked d and e, have $\Gamma = -1$ and 1 with degeneracies of 2 and 1 respectively. These also exhibit a true level crossing, with d being lower than e near $x = 1$ and vice versa near $x = 0$. Finally, the state with $S = 2$ marked f has $\Gamma = 1$ and is nondegenerate.

The composition of these six states can be easily understood at the noninteracting point $x = 1$. At this point, the ordering of energies is given by a $<$ d $<$ b $=$ e $=$ f $<$ c. The ground state a is the empty state. State d contains a single Majorana fermion with spin 1, with momentum equal to either π/L or $\pi - \pi/L$; hence the double degeneracy. The state b contains two fermions in a spin-0 combination, one with momentum π/L and the other with momentum $\pi - \pi/L$; hence the total momentum is π. States e and f have the same composition as b, except that they have spins 1 and 2 respectively. State c has three fermions in a spin-0 combination, two with momenta π/L and $\pi - \pi/L$, and the third with momentum either $3\pi/L$ or $\pi - 3\pi/L$; the double degeneracy is due to the twofold choice for the third fermion. If we now move from $x = 1$ to $x = 0$, all of these states get 'dressed' with an even number of fermions. At $x = 0$, the energy ordering is a = b = c < d = e < f.

Although the system sizes are not large, we can draw the following qualitative conclusions from these figures. First, the states evolve smoothly from $x = 0$ to $x = 1$ with no abrupt changes in between. In each spin sector, the lowest-energy states at $x = 0$ are mainly composed of the lowest-energy states at $x = 1$, and vice versa. Finally, the complex pattern of level crossings for small values of S seems to suggest that the model is nonintegrable for x not equal to 0 or 1.

5.2. Conformal field theory: a conjecture

It would be useful to understand the low-energy excitations of the model in terms of conformal field theory; amongst other things, this would lead to a simpler derivation of various correlation functions (see reference [12] and references therein). We would like to advance a conjecture in this direction. Before doing that, we must consider the two limits of the Hamiltonian (44) which are exactly solvable.

For $x = 1$, we have three uncoupled Majorana fermions with the same dispersion (15). The low-energy excitations (modes with momenta q close to 0 or π) have velocity $t = 4$ and are governed by a conformal field theory which is an $\mathrm{SU}(2)_2$ Wess–Zumino–Witten (WZW) model with central charge $c = 3/2$.

For $x = 0$, the unphysical states decouple completely. The physical states (each of which have an unphysical degeneracy of $2^{[L/2]}$ due to the spinless Majorana field ψ_n) are solvable by the Bethe *ansatz*; the low-energy physical excitations have the velocity $\pi J/2 = 2\pi$ and are governed by an $\mathrm{SU}(2)_1$ WZW conformal field theory with $c = 1$. The $x = 0$ limit is somewhat singular due to the complete decoupling of the unphysical states. Let us therefore examine what happens if x is nonzero but small. We can then apply degenerate perturbation theory to first order in x. For instance, consider perturbation theory amongst the $2^{[L/2]}$ ground states which are degenerate for $x = 0$; we denote these states by the direct product $|\Psi_0\rangle \otimes |\alpha\rangle$, where Ψ_0 is the physical ground state and α can take $2^{[L/2]}$ values. By rewriting $\boldsymbol{\phi}_n = \boldsymbol{\sigma}_n \psi_n$ and using the Bethe *ansatz* value

$$e \equiv \langle \Psi_0 | \boldsymbol{\sigma}_n \cdot \boldsymbol{\sigma}_{n+1} | \Psi_0 \rangle = -1.7726 \tag{45}$$

we find that the first term in the Hamiltonian (13) can be written as the perturbation

$$V = -\mathrm{i}xe \sum_n \psi_n \psi_{n+1}. \tag{46}$$

This can be diagonalized by Fourier transforming, as

$$\psi_n = \sqrt{\frac{2}{L}} \sum_{0<q<\pi} [c_q^\dagger \mathrm{e}^{\mathrm{i}qn} + c_q \mathrm{e}^{-\mathrm{i}qn}]. \tag{47}$$

Then

$$V = -4xe \sum_{0<q<\pi} \sin q \, c_q^\dagger c_q + \frac{2Lxe}{\pi}. \tag{48}$$

Thus the spinless sector with Z_2 charge has low-energy excitations with velocity $-4xe$. These are described by a conformal field theory with $c = 1/2$. Thus the spin and charge excitations have completely different velocities.

The question now is what happens in between the two limits. Although our numerical results are limited to $L = 4$ and 6, they suggest that both the spin sector (for instance, states with $S > 0$ and $\Gamma = 1$) and the charge sector (states with $S = 0$ and $\Gamma = -1$) remain gapless for all values of x; there does not appear to be a quantum phase transition at any point between $x = 0$ and 1. It is then natural to conjecture that the low-energy sector is generally described by the product of two conformal field theories which have different velocities; the spin sector by an $SU(2)_1$ WZW model with $c = 1$, and the Z_2 charge sector by a single Majorana fermion with $c = 1/2$. If this is correct, it would be somewhat reminiscent of the one-dimensional Hubbard model away from half-filling; the low-energy excitations of this are governed by the product of two conformal field theories which have different velocities if the on-site interaction $U \neq 0$; the spin sector is again described by an $SU(2)_1$ WZW model while the U(1) charge sector is described by a Gaussian field theory with $c = 1$ [12, 13].

6. The SO(N) t–J model

It is possible to generalize the t–J model with three species of Majorana fermions to a model with N species. In terms of an interpolating parameter x, we can write an SO(N)-symmetric Hamiltonian in the form

$$H = -\mathrm{i}x \sum_n \sum_{a=1}^{N} \phi_n^a \phi_{n+1}^a - (1-x) \sum_n \sum_{1\leqslant a<b\leqslant N} \phi_n^a \phi_n^b \phi_{n+1}^a \phi_{n+1}^b \tag{49}$$

where the operators ϕ_n^a satisfy the same anticommutation relations as in (2), except that the flavour indices a, b can now take N values. The Hilbert space for L sites has the dimensionality $2^{NL/2}$ if L is even. For $x = 1$, we have N noninteracting Majorana fermions with the dispersion $\omega_q = 4\sin q$; the low-energy excitations are therefore described by a $c = N/2$ conformal field theory. We will now examine two special cases, $N = 2$ and $N = 4$, for which the antiferromagnetic limit $x = 0$ is also well understood.

For $N = 2$, the model is equivalent to the XXZ spin-$\frac{1}{2}$ chain. This can be shown as follows. We first combine two Majorana operators to produce an annihilation operator for a spinless Dirac fermion:

$$d_n = \frac{(-\mathrm{i})^n}{2}(\phi_n^1 + \mathrm{i}\phi_n^2). \tag{50}$$

These satisfy the anticommutation relation

$$\{d_m, d_n^\dagger\} = \delta_{mn}. \tag{51}$$

In terms of these, the Hamiltonian takes the form

$$H = 2x \sum_n (d_n^\dagger d_{n+1} + d_{n+1}^\dagger d_n) + 4(1-x) \sum_n \left(d_n^\dagger d_n - \frac{1}{2}\right)\left(d_{n+1}^\dagger d_{n+1} - \frac{1}{2}\right). \tag{52}$$

A Jordan–Wigner transformation from fermions to spin-$\frac{1}{2}$ operators then produces the XXZ Hamiltonian [12]

$$H = x \sum_n (\sigma_n^x \sigma_{n+1}^x + \sigma_n^y \sigma_{n+1}^y) + (1-x) \sum_n \sigma_n^z \sigma_{n+1}^z. \tag{53}$$

This model is exactly solvable by the Bethe *ansatz* for all values of x; it has a quantum phase transition at $x = 1/2$. For $1/2 \leqslant x \leqslant 1$, the model is gapless and is described by a $c = 1$ Gaussian conformal field theory (the symmetry is enhanced from U(1) to SU(2) at $x = 1/2$). For $0 \leqslant x < 1/2$, the model is gapped and has a Néel ground state with long-range order.

The case of $N = 4$ is more interesting. At $x = 0$, the model is a direct sum of two antiferromagnetic spin-$\frac{1}{2}$ chains. To show this, let us first define the six generators of SO(4) at each site:

$$K_n^{ab} = \frac{\mathrm{i}}{2}\phi_n^a\phi_n^b. \tag{54}$$

Now we use the homomorphism $\mathrm{SO}(4) \simeq \mathrm{SO}(3) \times \mathrm{SO}(3)$. This can be proved by defining the linear combinations

$$\begin{aligned} L_{1n}^x &= \frac{1}{2}(K_n^{23} + K_n^{14}) \qquad & L_{2n}^x &= \frac{1}{2}(K_n^{23} - K_n^{14}) \\ L_{1n}^y &= \frac{1}{2}(K_n^{13} - K_n^{24}) \qquad & L_{2n}^y &= \frac{1}{2}(K_n^{13} + K_n^{24}) \\ L_{1n}^z &= \frac{1}{2}(K_n^{12} + K_n^{34}) \qquad & L_{2n}^z &= \frac{1}{2}(K_n^{12} - K_n^{34}). \end{aligned} \tag{55}$$

These generate two commuting SO(3) algebras, namely,

$$[L_{\alpha m}^a, L_{\beta n}^b] = \mathrm{i}\delta_{\alpha\beta}\delta_{mn}\sum_c \epsilon^{abc} L_{\alpha m}^c \tag{56}$$

where $\alpha, \beta = 1, 2$ label the two algebras, $a, b, c = x, y, z$, and $\epsilon^{xyz} = 1$. We can define total angular momentum operators

$$L_\alpha^a = \sum_n L_{\alpha n}^a. \tag{57}$$

These commute with the Hamiltonian (49) for all values of x.

At a single site, the Hilbert space is four dimensional; the four operators ϕ^a can be chosen to be the γ-matrices used in Dirac's theory of the electron. One can verify that

$$\begin{aligned} \mathbf{L}_1^2 &= \frac{3}{8}(\mathbf{I} - \phi_1\phi_2\phi_3\phi_4) \\ \mathbf{L}_2^2 &= \frac{3}{8}(\mathbf{I} + \phi_1\phi_2\phi_3\phi_4). \end{aligned} \tag{58}$$

It is convenient to choose a representation in which these two operators are diagonal in the form of 2×2 blocks:

$$\begin{aligned} \mathbf{L}_1^2 &= \begin{pmatrix} 3/4 & 0 \\ 0 & 0 \end{pmatrix} \\ \mathbf{L}_2^2 &= \begin{pmatrix} 0 & 0 \\ 0 & 3/4 \end{pmatrix}. \end{aligned} \tag{59}$$

Thus the upper two components of the Hilbert space transform as the $(\frac{1}{2}, 0)$ representation of $(\mathbf{L}_1, \mathbf{L}_2)$, while the lower two components transform as $(0, \frac{1}{2})$. We now see that, for $x = 0$, the Hamiltonian for L sites has the block-diagonal form

$$H = \begin{pmatrix} H_1 & 0 \\ 0 & H_2 \end{pmatrix} \tag{60}$$

where the Hamiltonians H_1 and H_2 act on two separate 2^L-dimensional Hilbert spaces, each corresponding to a spin-$\frac{1}{2}$ chain. Here

$$H_\alpha = 2J\sum_n \mathbf{L}_{\alpha,n}\cdot\mathbf{L}_{\alpha,n+1} \tag{61}$$

for $\alpha = 1, 2$. We already know that this can be solved by the Bethe *ansatz*; the block-diagonal form of (60) implies that each eigenvalue will have a twofold degeneracy. Thus the SO(4) t–J model is exactly solvable at both $x = 0$ and 1, and one can investigate how the spectrum interpolates between the two. We will not pursue this here.

The Majorana fermions in the SO(4) model carry the spin quantum numbers $(L_1, L_2) = (\frac{1}{2}, \frac{1}{2})$. In this respect they may be closer in spirit to the Faddeev–Takhtajan spinons (which are spin-$\frac{1}{2}$ objects) than the Majorana fermions in the SO(3) model which carry spin 1. To show this more precisely, let us define two Dirac fermion operators in the SO(4) model as

$$\begin{aligned} d_{1n} &= \frac{(-\mathrm{i})^n}{2}(\phi_{1n} + \mathrm{i}\phi_{2n}) \\ d_{2n} &= \frac{(-\mathrm{i})^n}{2}(\phi_{3n} + \mathrm{i}\phi_{4n}). \end{aligned} \tag{62}$$

We can then verify that the particles created by $d_{1n}^\dagger$ and $d_{2n}^\dagger$ have the eigenvalues of the total angular momentum operators (L_1^z, L_2^z) equal to $(\frac{1}{2}, \frac{1}{2})$ and $(\frac{1}{2}, -\frac{1}{2})$ respectively. Thus, for the purely antiferromagnetic model with $x = 0$, a fermion operator acting on the ground state of, say, the L_1-chain will produce states which transform as spin $\frac{1}{2}$ under the operators $\mathbf{L}_1$; in addition, the states will carry a twofold internal quantum number coming from $\mathbf{L}_2$.

It is interesting to note that the hopping term (proportional to t) in the SO(4) Majorana model is identical to the hopping term in the Hubbard model of electrons. However, the four-fermion interactions are very different in the two models.

Before ending this section, we would like to mention that a H–F analysis of the SO(N) antiferromagnet has been performed in reference [14]. Their H–F decomposition differs from the one that we have used in section 2. Consequently they obtain a much higher value for the ground-state energy than us—namely, equation (10) for $N = 3$, and $-JN(N-1)/2\pi^2$ in general.

7. Discussion

We have studied a one-dimensional SO(3)-invariant t–J model with Majorana fermions. At the pure-J end, this describes the nearest-neighbour antiferromagnetic spin-$\frac{1}{2}$ chain, while at the pure-t end, we have three noninteracting fermions. We have done perturbative calculations to low order in the four-fermion interaction. We have also studied the model numerically by means of exact diagonalization of small systems. These studies provide a new perspective on the excitations of the spin-$\frac{1}{2}$ chain by relating it in an 'adiabatic' and rotationally invariant way to a model of free Majorana fermions. The low-energy excitations of the spin-$\frac{1}{2}$ chain can be thought of as being made up of a small number of Majorana fermions.

The field theoretic description of the low-energy excitations of the model remains unclear. We have suggested that these excitations are governed by a product of two conformal field theories which have entirely different symmetries. Numerical studies, particularly finite-size scaling ones, of much larger systems are required to test this scenario.

The SO(N) generalization of our model also deserves further study. The SO(4) case seems to be especially interesting because it provides yet another way of smoothly connecting a model of free fermions to a spin-$\frac{1}{2}$ antiferromagnet. The SO(4) model may also have applications to the problem of two coupled spin-$\frac{1}{2}$ chains [15].

Acknowledgment

DS thanks the Department of Physics and Astronomy, McMaster University, for hospitality enjoyed during part of this work.

References

[1] Shastry B S and Sen D 1997 *Phys. Rev.* B **55** 2988
[2] Vieira V R 1981 *Phys. Rev.* B **23** 6043
Tsvelik A M 1992 *Phys. Rev. Lett.* **69** 2142
Coleman P, Miranda E and Tsvelik A M 1994 *Phys. Rev.* B **49** 8955
Coleman P, Ioffe L B and Tsvelik A M 1995 *Phys. Rev.* B **52** 6611
[3] Martin J L 1959 *Proc. R. Soc.* A **251** 536
Casalbouni R 1976 *Nuovo Cimento* A **33** 389
Berezin F A and Marinov M S 1977 *Ann. Phys., NY* **104** 336
[4] Arovas D P and Auerbach A 1988 *Phys. Rev.* B **38** 316
Wen X G, Wilczek F and Zee A 1988 *Phys. Rev.* B **39** 11 413
Marston J B and Affleck I 1989 *Phys. Rev.* B **39** 11 538
Sarker S, Jayaprakash C, Krishnamurthy H R and Ma M 1989 *Phys. Rev.* B **40** 5028
Yoshioka D 1989 *J. Phys. Soc. Japan* **58** 32
Chandra P, Coleman P and Larkin A I 1990 *J. Phys.: Condens. Matter* **2** 7933
Chitra R, Rao S, Sen D and Rao S S 1995 *Phys. Rev.* B **52** 1061
[5] Abrikosov A A 1966 *Physics* **2** 5
Keiter H 1971 *Phys. Lett.* **36A** 257
[6] Mudry C and Fradkin E 1994 *Phys. Rev.* B **50** 11 409
[7] Mattis D C 1965 *Theory of Magnetism* (New York: Harper and Row)
[8] Kenan R P 1966 *J. Appl. Phys.* **37** 1453
Spencer H J and Doniach S 1967 *Phys. Rev. Lett.* **18** 994
[9] des Cloiseaux J and Pearson J J 1962 *Phys. Rev.* **128** 2131
[10] Yamada T 1969 *Prog. Theor. Phys. Japan* **41** 880
Johnson D and McCoy B M 1972 *Phys. Rev.* A **6** 1613
Faddeev L D and Takhtajan L A 1981 *Phys. Lett.* **85A** 375
[11] Müller G, Beck H and Bonner J C 1979 *Phys. Rev. Lett.* **43** 75
Müller G, Thomas H, Beck H and Bonner J C 1981 *Phys. Rev.* B **24** 1429
[12] Affleck I 1989 *Fields, Strings and Critical Phenomena* ed E Brezin and J Zinn-Justin (Amsterdam: North-Holland)
Tsvelik A M 1995 *Quantum Field Theory in Condensed Matter Physics* (Cambridge: Cambridge University Press)
[13] Woynarovich F 1989 *J. Phys. A: Math. Gen.* **22** 4243
Izergin A G, Korepin V E and Reshetikhin N Yu 1989 *J. Phys. A: Math. Gen.* **22** 2615
Frahm H and Korepin V E 1990 *Phys. Rev.* B **42** 10 553
Kawakami N and Yang S-K 1991 *J. Phys.: Condens. Matter* **3** 5983
[14] Foerster D and Triozon F 1996 *Preprint* cond-mat/9611138
Foerster D 1997 *Preprint* cond-mat/9701093
[15] Shelton D G, Nersesyan A A and Tsvelik A M 1996 *Phys. Rev.* B **53** 8521
Allen D and Senechal D 1997 *Phys. Rev.* B **55** 299